Battery Optimization for Power Systems: Feasibility and Optimality

Mazen Elsaadany and Mads R. Almassalkhi

Abstract—The deployment of battery energy storage systems (BESS) is necessary to integrate terawatts of renewable generation while supporting grid resilience and reliability efforts. Optimizing battery dispatch requires predictive battery models that accurately characterize the battery state of charge (SOC) to ensure that the battery operates within the energy and power limits and avoids unexpected saturation effects. Furthermore, most BESS are unable to simultaneously charge and discharge, which begets an additional, non-convex complementary constraint. This paper presents and compares recently developed predictive battery models that side-step the non-convexity while providing supporting analysis on modeling error and optimal parameter selection. Specifically, insights for four different predictive BESS formulations are presented, including non-linear, mixed-integer, linear convex relaxation, and linear robust formulations. Additionally, two two-stage approaches are also considered. Analysis is conducted on optimal parameter selection for two of the methods, as well, as providing a new and improved SOC error bound on the relaxed formulation and the role of sustainability constraints on the robust formulation. Through the lens of relevant BESS use-cases, the paper discusses optimality and feasibility guarantees between the different models and provides extensive simulation-based analysis.

Index Terms—Battery, energy storage, modeling, optimization, convex, power systems

I. Introduction

Increased distributed energy penetration in the power grid will lead to lower system inertia, larger sensitivity to power imbalances and reduced system reliability [1]. The deployment of battery energy storage systems (BESS) promises to increase grid reliability and resilience especially with increased intermittent generation from renewable sources [2]. Proper modeling is needed for the optimal coordination and dispatch of BESS. The BESS models would need to characterize the charging power consumed, discharging power supplied, state of charge (SOC) and ensure that the BESS remains within its power and energy limits. Furthermore, BESS's, for the most part, are not capable of charging and discharging simultaneously. Therefore, an exact BESS model would require non-convex complementary constraint to ensure a physically realizable solution [3]. Different exact an non-exact BESS models are presented in the literature and have been used in a variety of applications. Exact BESS models enforce the non-convex complementary constraint; therefore, any solution is physically realizable and model SOC is accurate representation of BESS SOC. The complementary constraint can be modeled as a non-linear equality constraint as shown in [2], [4]. However, due to the non-convexity there is no guarantee of a globally optimal solution. Relaxing the complementary constraint and using the resulting solution as a warm start in the non-linear BESS model may help improve performance. The complementary constraint can also be satisfied by introducing a binary integer variable turning the problem into a Mixed Integer Program

(MIP) [4], [5] MIP models can make use of more advance MIP solvers that usually come at a high computational cost. Non-exact BESS models, on the other hand, side-step the complementary constraint and any simultaneous charging and discharging is implemented by considering the net power sequence (difference between charging and discharging sequence). The complementary constraint is relaxed in return for convex and less computationally taxing model [2], [4]. One main issue with non-exact BESS models is that the model SOC and realized BESS SOC, obtained by implementing the net power schedule, will not match due to the simultaneous charging and discharging. This may cause the BESS to reach its energy limits sooner than predicted by the non-exact model [6]. Therefore, some power schedules obtained from non-exact models may not be not physically realizable. In the context of this paper, a physically realizable power schedule indicates that the net power schedule can be applied to a BESS without any power or energy limit violations. Authors in [7], [8] give conditions under which the complementary constraint can be relaxed and simultaneous charging and discharging would be sub-optimal. In [6], a robust convex linear model is presented which ensures realized BESS SOC remains within energy limits by constraining upper and lower bounds on realized SOC. A two stage approach presented in [1], relaxes the complementary constraint and uses resulting solution trajectory to force either charging or discharging at each time step. BESS models have been used in a variety of applications. In [9], a linear BESS model is used in a model predictive control (MPC) scheme to find the optimal dispatch schedule of a BESS based on day ahead forecasts and real time updates. The complementary constraint is relaxed; however, an upper and lower bound on SOC (problem specific bounds) are constrained to be within the energy limits of the BESS and, thus, ensuring actual SOC remains within energy limits. In [10], optimal BESS dispatch is found allowing for simultaneous participation is day ahead, frequency regulation and energy reserve markets. The complementary constraint is relaxed in [11] and robust optimization framework is provided to deal with uncertainties in the energy, reserve and regulation markets. BESS models are also used in photovoltaic (PV) smoothing applications where the goal is to reduce the fluctuations in intermittent PV power generation [12], [13]. Imperfect PV data predictions are used in [14], along with an MPC scheme to optimize a multi-objective problem which aims to minimize fluctuations in PV generation, minimize excessive charge/discharge cycles (battery degradation) and maximize revenue through energy arbitrage. Operational cost of PV electric vehicle (EV) charging stations was optimized using an non-exact BESS model along with a multi-stage optimization framework and day ahead solar and energy prices forecasts [15]. Four BESS models are presented in this paper, a non-linear (NLP), a mixed integer (MIP), a convex relaxation (relaxed) and robust model formulation. Also, two two-stage models, non-linear with warm start (NLP-WS) and two-stage linear models are presented. The main contributions of this paper is as follows:

M. Elsaadany (Corresponding author) and M. Almassalkhi are both with the Department of Electrical and Biomedical Engineering at the University of Vermont, Burlington, VT. {melsaada,malmassa}@uvm.edu
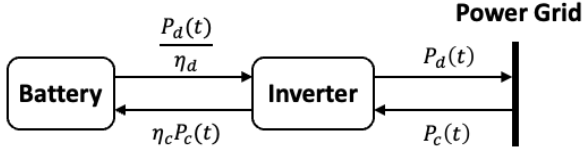
Figure 1. BESS block diagram with charging and discharging modes.

Figure 2. Predictive BESS model and physical implementation

- Insights into (sub)optimality, feasibility, realizability, and scalability of six different predictive battery formulations are presented.
- Derivation of a new, less conservative bound on worst-case SOC modeling error for the commonly used relaxed BESS optimization formulation.
- Analysis of optimal parameter selection in the robust and two-stage linear methods.
- Extensive simulation-based analysis of optimality and feasibility of the solutions of the different predictive BESS formulations for three relevant practical use-cases.

The rest of the paper is organized as follows: Section II presents and discusses the different BESS models. Section III discusses the analysis done on the error in the relaxed and robust models (non-exact models). Section IV discusses the simulations that were done and the use cases used to exemplify the differences in the BESS models. Section V presents the simulation results along with discussion and Section VI concludes the paper.

II. BATTERY OPTIMIZATION METHODS

In this section, different BESS formulations are presented and discussed. Fig. 1 shows a block diagram describing the basic structure of a BESS, where $P_c(t), P_d(t) \in [0,\bar{P}]$ are the battery inverter's charging and discharging powers at time t, respectively. Parameters $\eta_c, \eta_d \in (0,1]$ are the inverter's charging and discharging efficiencies, respectively. The initial battery SOC is denoted $E_0 \in [\underline{E},\bar{E}]$. From the diagram, it is clear that for the BESS model to supply a power of $P_d(t)$ to the power grid, it would need to discharge $\frac{P_d(t)}{\eta_d} \geq P_d(t)$ to account for the power losses. Similarly, if the BESS draws $P_c(t)$ from the grid, the battery only receives $\eta_c P_c(t) \leq P_c(t)$. Thus, there exists an inherent asymmetry between charging and discharging when $\eta_c, \eta_d < 1$. As seen in Fig. 1, on the inverter/AC side, the asymmetry is no longer present, therefore, simultaneous charging and discharging and the net power schedule are equivalent. However, on the battery side simultaneous charging and discharging, due to the asymmetry, is not equivalent to applying the net power schedule. At the end of the day, the battery will either charge or discharge (but not both). Therefore, a constraint, $P_c(t)P_d(t)=0$, is needed to ensure that resulting power schedule solutions do not contain simultaneous charging and discharging. The battery's continuous-time SOC trajectory then evolves along the manifold given by $P_c(t)P_d(t)=0$ and is defined as follows:

$$E(t) = E_0 + \int_0^t \eta_c P_c(\tau) - \frac{1}{\eta_d} P_d(\tau)d\tau. \qquad (1)$$

The continuous-time model in (1) is discretized with sampling time Δt. Zero-order hold sampling is used, i.e. $P_{c,d}(t) =: P_{c,d}[k] \quad \forall t \in [k\Delta t,(k+1)\Delta t)$ is constant within a single timestep, to yield the difference equation

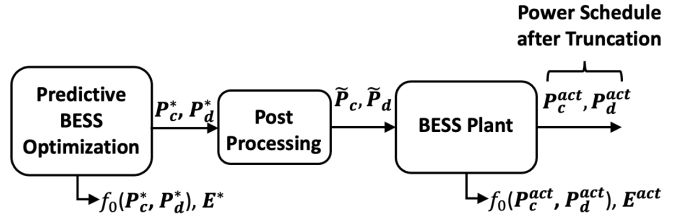$$E[k] = E_0 + \Delta t \sum_{n=0}^{k-1} \eta_c P_c[k] - \frac{1}{\eta_d} P_d[k]. \qquad (2)$$

constrained on nonlinear $P_c[k]P_d[k]=0$. We now want to optimize the power schedules over prediction horizon $k=0,...,K$, and find $\mathbf{P}_c^*,\mathbf{P}_d^* \in \mathbb{R}^K$.

Specifically, we analyze herein the optimality, feasibility, and computational aspects of six different (commonly used) battery optimization approaches from literature: four optimization formulations and two bi-level optimization schemes. The formulations include the exact, non-convex non-linear (NLP) and equivalent mixed integer (MILP) formulations, as well as a commonly employed convex relaxation and a new robust linear model. In addition to stand-alone formulations, we consider a warm-start relaxed-NLP (NLP-WS) implementation and a two-stage linear scheme that employs thresholding to sidestep complementarity conditions. The relaxed and robust models do not explicitly include the complementary constraint and, therefore, may result in solutions with *simultaneous charging and discharging* (i.e., $P_c^*[k]P_d^*[k] > 0$). As illustrated in Fig. 2, a BESS can only implement a single input in practice, i.e., a BESS must post-process the net-charge command, $P_c^*[k]-P_d^*[k]$, according to

$$\tilde{P}_c[k] = \max\{P_c[k]-P_d[k],0\} \qquad (3a)$$
$$\tilde{P}_d[k] = \max\{P_d[k]-P_c[k],0\}. \qquad (3b)$$

This means that the effects of asymmetry in charging and simultaneous discharging, $P_c^*[k]P_d^*[k]>0$, result in an error between the predicted SOC trajectory, $\mathbf{E}^* \in \mathbb{R}^{K+1}$, and the realized SOC trajectory, $\mathbf{E}^{act} \in \mathbb{R}^{K+1}$. That is, with simultaneous charging/discharging, the predicted net-charging control schedule may not be realizable due to unexpected saturation in the SOC trajectory. This can lead to a realized performance in the plant, $f_0(\mathbf{P}_c^{act},\mathbf{P}_d^{act})$ that is worse than the predicted performance, $f_0(\mathbf{P}_c^*,\mathbf{P}_d^*)$, which can negatively impact long-term battery revenue, battery state of health, or grid reliability [16].

Note that the BESS plant enforces energy limits by truncating the commanded power schedule by setting $P_c^{act}(t) = 0$, when $E^{act}(t)=\bar{E}$. Similarly, if $E^{act}(t)=\underline{E}$ then $\tilde{P}_d(t)=0$. The resulting power schedule after truncation is denoted by $\mathbf{P}_c^{act}$ and $\mathbf{P}_d^{act}$ with the associated objective function value $f_0(\mathbf{P}_c^{act},\mathbf{P}_d^{act})$. Note that if the predictive model satisfies the complementary constraint, then $\mathbf{P}_c^*=\mathbf{P}_c^{act}$, $\mathbf{P}_d^*=\mathbf{P}_d^{act}$ and $f_0(\mathbf{P}_c^*,\mathbf{P}_d^*)=f_0(\mathbf{P}_c^{act},\mathbf{P}_d^{act})$.

Definition II.1. *Implementable solution/power schedule refers to a physically realizable power schedule $(\mathbf{P}_c,\mathbf{P}_d)$ whose net power schedule $(\mathbf{P}_{net} = \mathbf{P}_c - \mathbf{P}_d)$ can be applied to a BESS without violation of energy or power limits.*

The six different methods for battery optimization are presented next. The objective functions are omitted from discussion for now, but are convex and provided in Section IV.

A. Non-linear formulation

The NLP model formulation is given by

$$E[k+1] = E[k] + \Delta t \eta_c P_c[k] - \Delta t \frac{1}{\eta_d} P_d[k] \quad (4a)$$

$$E[0] = E_0 \quad (4b)$$

$$0 \leq P_c[k] \leq \overline{P} \quad (4c)$$

$$0 \leq P_d[k] \leq \overline{P} \quad (4d)$$

$$0 \leq E[k+1] \leq \overline{E} \quad (4e)$$

$$P_c[k] P_d[k] = 0 \quad (4f)$$

for $k = 0, \ldots, K$. The complementary condition is satisfied with the explicit non-convex constraint (4f), which makes the NLP non-convex. Since the formulation is non-convex, global optimality is not guaranteed and the resulting NLP formulation is NP-hard, which increases computational complexity. However, the benefit of adding (4f) is that any feasible solution to (4) is realizable.

B. Mixed-integer linear formulation

The complementary constraint in (4f) can be equivalently represented with binary variables to enforce either charging or discharging input to be zero. Thus, the resulting MIP model introduces a binary variable for each timestep and the formulation is given by

$$(4a), (4b) \text{ and } (4e) \quad (5a)$$

$$0 \leq P_c[k] \leq z[k]\overline{P} \quad (5b)$$

$$0 \leq P_d[k] \leq (1 - z[k])\overline{P} \quad (5c)$$

$$z[k] \in \{0, 1\}, \quad (5d)$$

for $k = 0, \ldots, K$ and where the binary variable is such that $z[k] = 1 \Rightarrow P_d[k] = 0, P_c[k] \in [0, \bar{P}]$.

The MIP formulation can leverage recent advances in MIP solvers to find "good" feasible solutions quickly, even though the MIP formulation is non-convex and NP-hard, in general. In addition, MIP formulations, whose integer-relaxed problem is convex, provide a valuable optimality gap from which we can gauge integer-feasible solution quality. However, finding the globally optimal solution comes at a high computational cost for large-scale problems (e.g., when $K \gg 1$ timesteps or $N \gg 1$ BESS units).

C. Convex Relaxation Linear BESS Model

A relaxed model is obtained directly from the NLP formulation in (4) by omitting (4f) altogether. The relaxed formulation employed herein is borrowed from [1], which adds a cutting plane to the formulation to reduce the effect of simultaneous charging and discharging and is given by

$$(4a) - (4e) \quad (6a)$$

$$P_c[k] + P_d[k] \leq \overline{P} \quad (6b)$$

for $k = 0, \ldots, K$. Clearly, the relaxed model allows simultaneous charging and discharging, so constraint (6b) is added and the post-processing given in (3) must be considered when implementing the optimal power schedule produced by (6) on a BESS plant. From [1], it is proven that the SOC obtained from the relaxed model is a lower bound on the realized SOC (i.e., obtained after post processing and truncation). Thus, the relaxed model's power schedule may cause unexpected saturation in the SOC, which can lead to sudden curtailment of the charging schedule. That is, the relaxed formulation sacrifices prediction accuracy for convexity, from which computational gains can be achieved. For a set of general conditions under which simultaneous charging and discharging will be sub-optimal is given in [1], [7], [8].
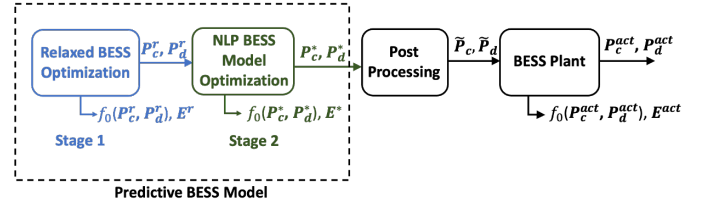

Figure 3. Two-stage NLP method with relaxed warm start

D. Two-stage method I: NLP with relaxed warm start

To improve the NLP's (locally optimal) performance, one can provide it with a good (warm) starting point. This warm start can be provided from the relaxed formulation in (6) as illustrated in Fig.3.

This results in a two-stage method and relies on the relaxed formulation to find a solution that is "close enough" to the global optimum. However, due to the non-convexity of the NLP, there is no guarantee that: (a) the two-stage method will solve quickly nor (b) that it will recover the globally optimal solution. However, the two-stage method will at least provide an optimality gap and feasibility of the relaxed solution can be checked before executing the NLP, which can reduce computational efforts under certain circumstances.

E. Two-stage method II: Linear with relaxed thresholding

Instead of sending the relaxed solution $(\mathbf{P}_c^r, \mathbf{P}_d^r)$ to a non-convex NLP, we could process the relaxed solution based on its optimized net-charging values (i.e., $P_{net}^r[k] := P_c^r[k] - P_d^r[k]$) and use that net value and a chosen threshold $\alpha \geq 0$ to lock variables for either charging (if $P_{net}^r[k] < -\alpha \Rightarrow P_c[k] = 0$) or discharging (if $P_{net}^r[k] > \alpha \Rightarrow P_d[k] = 0$) to zero. Then, based on the thresholding outcome, we re-run the relaxed problem, but with most/all complementarity conditions explicitly enforced for small enough α, which also reduces the dimension of the second-stage problem. This method is based on [1] and outlined in Algorithm 1 and illustrated in Fig. 4.

Clearly, the choice of α affects the number of timesteps that will be forced to either charging or discharging modes, which is discussed in Section III-D. In addition, the thresholding effectively reduces the feasible set of the augmented second-stage formulation, which speeds up the second-stage solve time, but can result in sub-optimal outcomes. Of course, sub-optimality comes with the benefit that as more complementarity conditions become enforced through thresholding, the second-stage optimal solution will become realizable.

Algorithm 1 Two-Stage method II: Linear BESS Model

1: Initialize: $\alpha \in [0, \overline{P}]$
2: Solve (6) and obtain $\mathbf{P}_c^r, \mathbf{P}_d^r \in \mathbb{R}^{K+1}$.
3: **for all** $k = 0, \ldots, K$ **do**
4:     **if** $P_c^r[k] - P_d^r[k] \geq \alpha$ **then**
5:         Add equality constraint $P_d[k] = 0$ to 2nd Stage Problem
6:     **end if**
7:     **if** $P_c^r[k] - P_d^r[k] < -\alpha$ **then**
8:         Add equality constraint $P_c[k] = 0$ to 2nd Stage Problem
9:     **end if**
10: **end for**
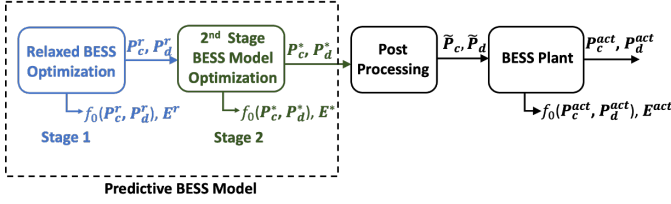11: Solve 2nd Stage Problem w/ added equality constraints in (6).

Figure 4. Two-stage linear method with thresholding

Figure 5. Qualitative comparison of different BESS formulations

F. Robust Linear Formulation

The relaxed model in (6) has the benefit of low computational burden and convexity; however, side stepping the complementary constraint can lead to implementation issues. The two-stage method in Algorithm 1 offered a different convex approach, but requires almost double the computation time and solution may not guarantee realizability (depending on choice of α). Thus, we are interested in a single convex formulation with realizability guarantees. In [6], a convex envelope is constructed that provably contains the actual SOC trajectory at all times and the convex envelope is then constrained to lie within the SOC limits. This leads to a robust formulation with conservative (sub-optimal) solution. We borrow this robust method, which is given by

$$E_{\text{UB}}[k+1] = E_{\text{UB}}[k] + \Delta t \eta (P_c[k] - P_d[k]) \tag{7a}$$

$$E_{\text{LB}}[k+1] = E_{\text{LB}}[k] + \Delta t \eta_c P_c[k] - \Delta t \frac{1}{\eta_d} P_d[k] \tag{7b}$$

$$E_{\text{LB}}[0] = E_0 \tag{7c}$$

$$E_{\text{UB}}[0] = E_0 \tag{7d}$$

$$(4c) \text{ and } (4d) \tag{7e}$$

$$E_{\text{UB}}[k+1] \le \overline{E} \tag{7f}$$

$$E_{\text{LB}}[k+1] \ge 0 \tag{7g}$$

for $k = 0,...,K$, where the upper/lower SOC "proxy" trajectories are given by $E_{\text{UB/LB}}$ and parameter $\eta \in [\eta_c, 1/\eta_d]$ is chosen a-priori. In Section III-B, we analytically derive the optimal choice for η. Note that (7) does not explicitly predict the actual SOC, but instead finds the optimal net power commands for which the envelope satisfies the SOC limits, which guarantees that the actual SOC under the same net power command does too.

Remark (Sustainability constraints). *Note that the robust model only characterizes the SOC envelope that contains the actual SOC trajectory and not a prediction of the actual SOC. Therefore, implementing a terminal "sustainability" constraints on the SOC (e.g., $E[K] = E_0$) is not straightforward. Including the terminal constraint $E_{LB}[K] = E_0$ would ensure $E^{act}[K] \ge E_0$, while $E_{UB}[K] = E_0$ would guarantee $E^{act}[K] \le E_0$. Separately, these may be acceptable terminal conditions for certain applications. Enforcing both conditions, however, can lead to infeasibility or suboptimal outcomes as presented in Section III-C.*

There is a tradeoff between the BESS model formulations as illustrated in Fig. 5 . Accurate formulations, such as the NLP or MIP, come at the cost of poor quality of solution (NLP since non-convex) and/or large computational burden. Relaxed has low computational burden but yield solutions that may not be physically realizable especially for net-charging sequence which may cause the BESS to reach the upper SOC limit sooner than predicted by the relaxed

model. The robust models also has a lower computational burden but yields solutions that may be conservative/sub-optimal due to a limited feasible set. The choice of η affects how the feasible set is limited, hence the need for an optimal choice of η that yields the least sub-optimal solution. NLP-WS comes with a larger computational burden than NLP and with no guarantee of improved solution (since still non-convex). The two-stage linear model, for an appropriate choice of α is an accurate model that improves on the relaxed model but comes with the need of solving two sub-problems instead of one.

III. ANALYTICAL RESULTS FOR BESS OPTIMIZATION

The previous section discussed four models (NLP, MIP, relaxed and robust models), as well as a couple two-stage models (NLP-WS and the Two-stage linear model). The relaxed model's predicted SOC is a lower bound on the realized SOC which may lead to implementation issues for net-charging sequences ($E[K] \ge E_0$). A bound on the error between relaxed model and realized BESS SOC is presented for charging sequence. The bound is then shown to be tighter than existing bounds such as the one presented in [6]. Furthermore, the previous section introduced the robust and two-stage linear models, each of which have model parameters η and α respectively. This section discusses the effect of these parameters on model performance and provides the optimal choice for η in the robust model.

A. Improved error bound for the relaxed formulation

The predicted SOC from the relaxed model is a lower bound on the realized SOC, $E^r[k] \le E[k]$, which can lead to unexpected saturation at the upper limit, $\overline{E}$. Thus, we are interested in how well the relaxed model predicts the SOC for net-charging input sequences. That is, consider a net-charging sequence at time k, i.e. $E^r[k] \ge E_0$. Then, the following recursive relation holds:

$$\eta_c \sum_{n=0}^{k-1} P_c[n] \ge \frac{1}{\eta_d} \sum_{n=0}^{k-1} P_d[n]. \tag{8}$$

Denote the error between relaxed and realized SOCs as $\Delta E[k] := E[k] - E^r[k]$, which can be expanded to give

$$\Delta E[k] = \Delta t (\frac{1}{\eta_d} - \eta_c) \sum_{n=0}^{k-1} \min\{P_c[n], P_d[n]\} \le \Delta t (\frac{1}{\eta_d} - \eta_c) \sum_{n=0}^{k-1} P_d[n], \tag{9}$$

where $P_d[n] \ge \min\{P_c[n], P_d[n]\}$. Combining (8) and (9), we get

$$\Delta E[k] \le \Delta t k \frac{\eta_c(1 - \eta_c \eta_d)}{1 + \eta_c \eta_d} \bar{P}, \tag{10}$$

which represents an error bound on largest error between relaxed and realized SOC for a net-charging sequence.

Proposition 1. *The SOC error bound from* (10) *is tighter than the error bound given in [6, (11)]: $\Delta \hat{E}[k] := \Delta t k (\frac{1}{\eta_d} - \eta_c) \frac{\bar{P}}{2}$.*

Proof. The difference between the two bounds is given by

$$\Delta \hat{E}_c[k]\Delta - \overline{E}[k] = \Delta t k \frac{\overline{P}}{2}\left(\frac{(1-\eta_c\eta_d)^2}{\eta_d(1+\eta_c\eta_d)}\right) \geq 0. \qquad (11)$$

Since the difference is non-negative this completes the proof. $\square$

Thus, the SOC error bound in (10) is tighter that the bound from [6], which applies to any application with the relaxed formulation.

B. Optimal parameter selection for robust formulation

The conservativeness in the robust model's upper SOC trajectory $\mathbf{E}_{UB}$ is a function of the choice of η. Thus, we are interested in finding the η that minimizes the difference between $\mathbf{E}_{UB}$ and the (lower) realized SOC trajectory, $\Delta E_{UB}[k] := E_{UB}[k] - E[k]$, to reduce conservativeness. Specifically, we want to find the η such that when $E_{UB}[k] = \overline{E}$, $\Delta E_{UB}[k]$ is minimized.

Proposition 2. *The optimal η in the robust formulation (7) is η_c.*

Proof. Consider an $\mathbf{E}_{UB}$ trajectory arriving at its upper limit at time l, i.e., $E_{UB}[l] = \overline{E}$. Then, it must have been subject a net-charging input sequence, i.e., $\sum_{k=0}^{l}(P_c[k]-P_d[k]) \geq 0$. Then, the SOC error, $\Delta E_{UB}[l]$, is given by the following:

$$\Delta E_{UB}[l] = \Delta t \sum_{k=0}^{l-1}(\eta-\eta c)\max\{P_c[k]-P_d[k],0\}$$
$$+ (\frac{1}{\eta_d}-\eta)\max\{P_d[k]-P_c[k],0\} \qquad (12)$$

$$\Rightarrow \frac{\partial \Delta E_{UB}[l]}{\partial \eta} = \Delta t \sum_{k=0}^{l-1}(P_c[k]-P_d[k]) \geq 0. \qquad (13)$$

Thus, in (13), if $\frac{\partial \Delta E_{UB}[l]}{\partial \eta} > 0$, then by decreasing η, one would decrease $\Delta E_{UB}[l]$. This means that the optimal choice of η is at its lower bound, which is η_c. For $\frac{\partial \Delta E_{UB}[l]}{\partial \eta} = 0$, the choice of η does not have an effect on $\Delta E_{UB}[l]$. This completes the proof. $\square$

From this result, we can guarantee a least conservative robust formulation with $\eta = \eta_c$, which is used in Section V.

C. Analysis of terminal SOC constraints in robust formulation

To expand on the remark on sustainability constraints in Section II-F, consider a terminal constraint on SOC of the form $E_{UB}[K] = E_f = E_{LB}[K]$ with $E_f \geq 0$. Then, the following holds.

Proposition 3. *For any $\eta \in [\eta_n, 1/\eta_d]$ with $\eta_c < 1/\eta_d$, adding terminal constraint $E_{UB}[K] = E_f = E_{LB}[K]$ to (7) will either result in infeasibility, a trivial solution $P_c^*[k] = 0 = P_d^*[k] \quad \forall k$ or satisfy complementarity conditions by halving the feasible set.*

Proof. From (7a) and (7b) and the terminal constraint at time K, we can recursively relate the upper and lower bound trajectories via the inputs P_c, P_d as

$$\sum_{k=1}^{K}(\eta-\eta_c)P_c[k] + \left(\frac{1}{\eta_d}-\eta\right)P_d[k] = 0. \qquad (14)$$

Thus, the following cases arise:
- With $\eta_c < 1/\eta_d$ and $\eta \in (\eta_c, 1/\eta_d)$ then $(\eta-\eta_c),(1/\eta_d-\eta) > 0$, which reduces the feasible set to $P_c[k] = 0 = P_d[k] \quad \forall k$, if $E_f = E_0$, and the robust formulation is infeasible, if $E_f \neq E_0$.
- With $\eta_c < 1/\eta_d$ and $\eta = \eta_c$ (or $\eta = 1/\eta_d$), then $P_c[k] \geq 0$ and $P_d[k] = 0$ (or $P_c[k] = 0$ and $P_d[k] \geq 0$) for all k, which satisfies complementarity conditions but cuts the feasible set in half. Thus, the robust formulation is only feasible if $E_f \geq E_0$ (or $E_f \leq E_0$)

since SOC trajectories are restricted to be monotonically increasing (or decreasing) and will be sub-optimal.

$\square$

The trivial case of $\eta_c = 1 = \eta_d$ was excluded above since it begets $\eta = 1$, which means that any solution $P_c^*[k], P_d^*[k]$ will be trivially implementable and satisfy the terminal SOC constraint. Thus, the interactions between terminal SOC constraint, E_f, η, and η_c, η_d are subtle, yet have a large impact on feasibility of the robust model.

D. Analysis of thresholding parameter in 2-stage linear scheme

The performance of the two-stage linear in Algorithm 1 is $f_0(\mathbf{P}_c^*, \mathbf{P}_d^*)$ and employs a thresholding parameter $\alpha \geq 0$ to lock many decision variables $P_c[k], P_d[k]$ to zero in the second stage to mitigate the effect of relaxing the complementarity constraint (4f). The smaller α, the more variables are locked in the second stage, which restricts the feasible set of the second stage. Thus, the method's predicted performance, $f_0(\mathbf{P}_c^*, \mathbf{P}_d^*)$, is a non-increasing function of α. For example, if $\alpha \geq \max_k\{|P_c^r[k]-P_d^r[k]|\}$, then none of the second-stage decision variables are locked and the second stage problem returns the solution from the first relaxed stage. If $\alpha \leq \min_k |P_c^r[k]-P_d^r[k]|$, then all decision variables are locked in the second stage, which satisfies complementarity constraint (4f). Let $f_0(\mathbf{P}_c^{r,act}, \mathbf{P}_d^{r,act})$ denote the BESS plant performance from the relaxed model is used.

Proposition 4. *If $\alpha \leq \min_k\{|P_c^r[k] - P_d^r[k]|\} \quad \forall k$ then $f_0(\mathbf{P}_c^{act}, \mathbf{P}_d^{act}) \leq f_0(\mathbf{P}_c^{r,act}, \mathbf{P}_d^{r,act})$*

Proof. The relaxed model solution is implemented on the plant as $\mathbf{P}_c^{r,act}$ and $\mathbf{P}_d^{r,act}$ after post-processing and truncation, which eliminates simultaneous charging/discharging and truncates power commands (if necessary) to ensure that SOC limits are satisfied. Hence, $\mathbf{P}_c^{r,act}, \mathbf{P}_d^{r,act}$ represents a feasible solution in stage two of the problem, so $f_0(\mathbf{P}_c^*, \mathbf{P}_d^*) \leq f_0(\mathbf{P}_c^{r,act}, \mathbf{P}_d^{r,act})$. However, with α small enough, all timesteps satisfy complementarity condition and, thus, the second-stage optimal solution is implementable, i.e., $f_0(\mathbf{P}_c^*, \mathbf{P}_d^*) = f_0(\mathbf{P}_c^{act}, \mathbf{P}_d^{act})$, which completes the proof. $\square$

Proposition 4 guarantees that, for $\alpha = 0$, the realized performance of the two-stage linear model is no worse than the realized performance of the relaxed model. Thus, we use $\alpha = 0$ in the next section.

IV. POWER SYSTEM BATTERY USE-CASES

Three use cases are considered with the different BESS optimization methods to characterize optimality (quality of solution), computational burden and implementability of the solution. The use cases are: 1) Power Reference Tracking, 2) PV Smoothing and 3) Revenue Maximization and are discussed next.

A. Power Reference Tracking

This use case involves finding the optimal charging/discharging dispatch schedule of a BESS to minimize mean-squared tracking error (MSE) with respect to a reference power signal (P_{ref}). In many power system applications, a BESS will need to track a given reference signal. The reference power signal can be based on day-ahead market forecasts and/or real time corrections. The objective function used is shown below:

$$\min \sum_{k=0}^{K}((P_c[k]-P_d[k])-P_{ref})^2. \qquad (15)$$

In this use case, we consider the MSE along with the solve times as metrics to evaluate optimality of the solutions and the computational

burden of the different models. Note, that in the case of the relaxed model, the optimal power commands may not always be realizable. Therefore, the relaxed formulation can over-estimate its level of performance and under-deliver due to (unexpected) saturation issues. Hence, the predicted and realized MSE for each model are obtained and used along with the solver times to evaluate the performance of the models. The reference signal is obtained from PJM's Reg-D historical data [17].

B. PV Smoothing

In this use case a BESS is co-located with solar PV and dispatched to smooth out expected fluctuations PV power generation. Given a forecast of PV power generation (P_{PV}), the goal is to find the optimal dispatch schedule to minimize the ramps in the net PV power ($P_{\mathrm{PV}} - P_{\mathrm{c}} + P_{\mathrm{d}}$). The solar data was obtained form [18] and the objective function used is

$$\min \sum_{k=0}^{K} [(P_{\mathrm{PV}}[k+1] - P_{\mathrm{c}}[k+1] + P_{\mathrm{d}}[k+1]) \quad (16)$$
$$- (P_{\mathrm{PV}}[k] - P_{\mathrm{c}}[k] + P_{\mathrm{d}}[k])]^2.$$

Note that the objective function takes the difference of the net PV power between two consecutive timesteps, i.e., the ramp in the net PV power. The objective function minimizes the sum of ramps squared. The MSE between the net PV power and the mean PV power is used as a metric to evaluate optimality and feasibility of the different solutions as well as the computational burden of the different models. Furthermore, another metric known as the R_{99} metric is used to evaluate the performance [19]. R_{99} metric is the 99th percentile of the ramps in net PV output. The R_{99} metric gives a sense of the maximum ramps in the smoothed PV output and the MSE metric gives an sense of the overall PV smoothing over all timesteps.

C. Revenue Maximization

Given an energy price signal, such as the day ahead market price forecasts [15] or NY-ISO 3-hour ahead forecasts, the battery dispatch should be such to maximize revenue gained from supplying (discharging) energy to the grid and minimize the cost consuming (charging) energy from the grid. The objective function is

$$\min \sum_{k=0}^{K} \mathrm{LMP}[k](P_{\mathrm{c}}[k] + P_{\mathrm{demand}}[k] - P_{\mathrm{PV}}[k] - P_{\mathrm{d}}[k]), \quad (17)$$

which captures total revenue of supplying a load P_{demand} with co-located solar PV source P_{PV}. The solve time and the predicted and achieved revenues are used as metrics to asses the computation burden of the models and the optimality and feasibility of the solutions from each of the models. The LMP price data is obtained from [20]. A three hour window is considered to emulate the NY-ISO 3 hour ahead forecasts.

V. SIMULATION RESULTS AND DISCUSSION

The use cases discussed in the previous section are implemented using the BESS specifications obtained from [21]. The BESS specifications are summarized in Table. I.

A. Power Reference Tracking

The power reference tracking use-case was implemented and the predicted and actual MSE for each of the models is summarized in Table. II.

As expected the NLP model the worst in terms of optimality (highest MSE) and has a relatively large computational burden. The MIP

Table I
BESS PARAMETERS

Parameters	Value	Unit
Charge/discharge efficiencies, $\eta_{\mathrm{c}}/\eta_{\mathrm{d}}$	0.95	-
Maximum charge/discharge power, $P_{\max}$	5.00	kW
Maximum energy capacity, $\bar{E}$	13.0	kWh

Table II
POWER REFERENCE TRACKING MSE AND SOLVER TIME

Model	Solver Time (s)	Predicted MSE (kW^2)	Actual MSE (kW^2)
NLP	6.5750	1.5390	1.5390
NLP WS	1.962	0.0487	0.0487
MIP	60.000	0.0487	0.0487
Relaxed	0.016	0.0056	0.2265
Robust	0.016	0.0527	0.0527
Two-Stage LP	0.020	0.0488	0.0488

performs the best in terms of optimality (lowest MSE) yet the worst in terms of computational burden (highest solver time). The relaxed model predicts the best solution but when the solution is implemented the actual SOC saturates earlier than predicted at around t= 12 hrs (as can be seen in Fig. 6), indicating the power schedule obtained was not feasible/physically realizable. This causes the actual MSE to be significantly larger. The robust model yielded a more conservative solution but with the guarantee of no implementation issues. Both of the two-stage models (NLP-WS and two-stage linear) yield MSE similar to that of the MIP model and require a fraction of the computational cost.
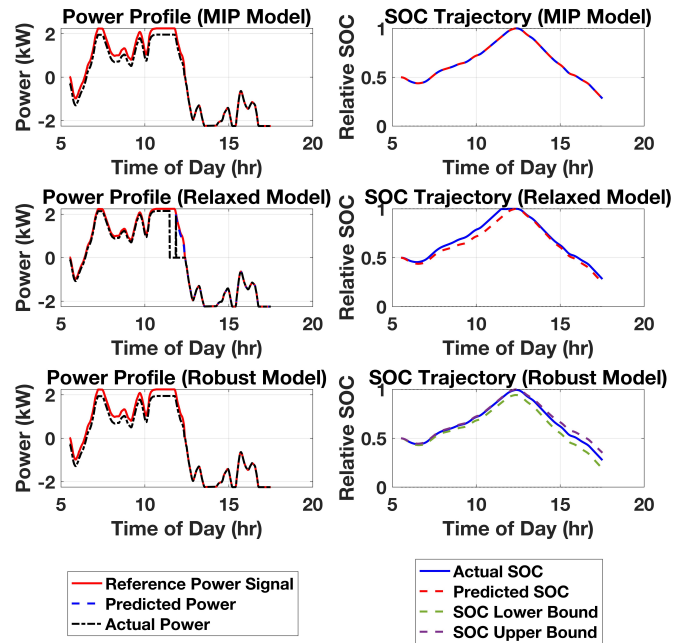

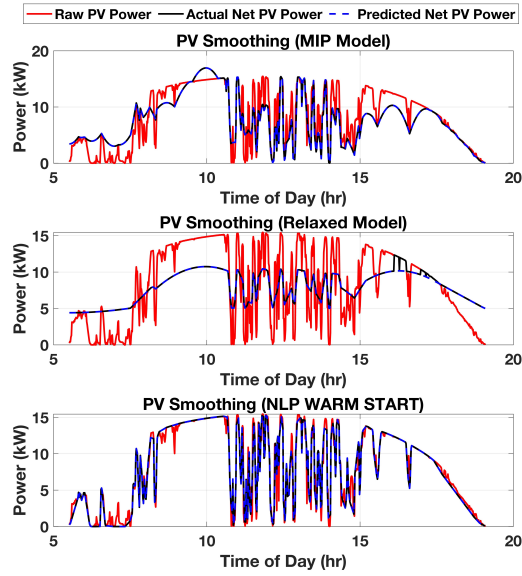Figure 6. Power Reference Tracking Power Profiles

Figure 7. PV Smoothing Net PV Output Profiles

Figure 8. Revenue Maximization BESS Dispatch

B. PV Smoothing

The PV smoothing use-case was implemented with the goal of minimizing the ramps in the net PV power output. The performance metrics for each of the models is summarized in Table. III. Similar (but not same) trends are seen as in the previous use case. The NLP model still delivers the the worst solution in terms of MSE, R_{99} and has the largest computational burden as seen by the solver time. The MIP model yields the best results overall in terms of MSE and R_{99} but comes with a larger solver time compared to the relaxed, robust and two-stage linear models. Similar to the previous use case, the relaxed model predicts the best results but falls short due to SOC saturation when the solution is implemented, as seen Fig. 7 by the sudden spikes in smoothed PV output at t=17hrs. The robust model gives a more conservative result as can be seen from the larger MSE. The non-linear model with the warm start actually yeilds a worse solution than NLP, showing that there is still no guarantee of optimality due to the non-convex nature of the problem. The two-stage linear delivers good performance (low MSE and R_{99}) outperformed only by the MIP model but the two-stage linear requires a fraction of the computational time

model is summarized in Table. IV. Similar to the other use-cases, the NLP model runs into local minima resulting in the worst solution (lowest revenue). Using the NLP-WS model improves the solution but still, better solutions (higher revenues) were achieved by the MIP and two-stage linear models. The MIP and two-stage linear models generate the highest revenue with the Twp-stage LP model requiring a fraction of the solver time. The relaxed model model predicts a larger revenue than what is actually achievable and the robust model gives a conservative yet implementable result.

Table IV
REVENUE MAXIMIZATION PERFORMANCE METRICS

Model	Solver Time (s)	Predicted Revenue ($)	Actual Revenue ($)
NLP	0.683	0.256	0.256
NLP WS	0.881	0.289	0.289
MIP	0.075	0.291	0.291
Relaxed	0.0016	0.291	0.284
Robust	0.0023	0.271	0.271
Two-Stage LP	0.0030	0.291	0.291

Table III
PV SMOOTHING PERFORMANCE METRICS

Model	Solver Time (s)	Predicted R99 (kW/min)	Actual R99 (kW/min)	Predicted MSE (kW^2)	Actual MSE (kW^2)
NLP	6.934	4.59	4.59	18.42	18.42
NLP WS	5.480	6.33	6.33	27.30	27.30
MIP	0.798	1.10	1.0	4.69	4.69
Relaxed	0.025	1.10	1.15	4.46	4.79
Robust	0.028	1.10	1.10	5.20	5.20
Two-Stage LP	0.037	1.10	1.10	4.72	4.72

C. Revenue Maximization

The revenue maximization use-case was implemented with a 3 hour price signal obtained from [20], the price signal has 5-min resolution. The predicted and actual revenue generated using each
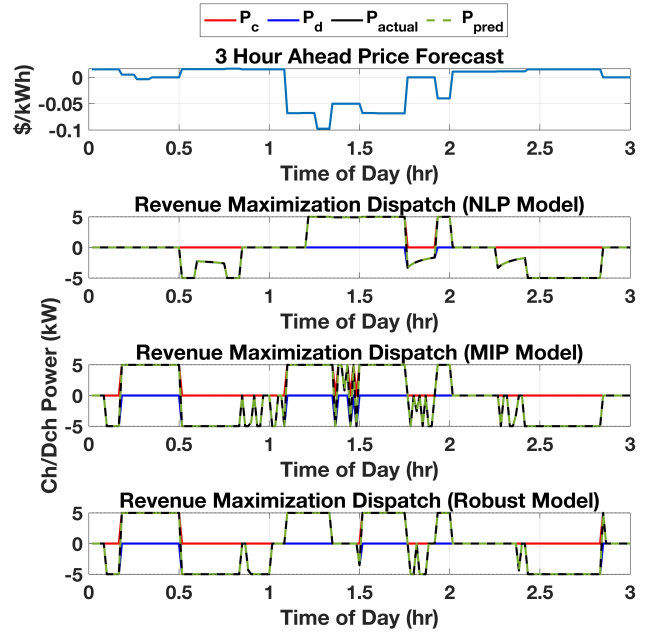
VI. CONCLUSION

This work gives key insight into the optimality, feasibility and computational burden of six commonly used BESS formulations which were then backed up by simulation results. The NLP model, due to its non-convex nature, was seen to frequently run into local minima, resulting in sub-optimal solutions. Using a warm start (NLP-WS) was seen to improve solutions but not in all use-cases, showing that the solution improvement is not guaranteed. The relaxed formulation is convex and is the least computationally taxing; however, may produce a charge/discharge trajectory that is not physically realizable since predicted SOC is a lower bound on realized SOC. For a power schedule that leads to an increase in SOC and potentially implementation issues, a bound on the error in predicted SOC is found. The bound is then

shown to be tighter than ones presented in literature. The effect of the choice of parameter α in the two-stage linear formulation is discussed. It was shown, for an appropriate choice of α, the realized performance of the two-stage linear formulation is no worse than that of the relaxed formulation. The two-stage linear was seen to improve performance of the relaxed model and eliminate any implementation issues. However, it requires solving two sets of problems which may be taxing for larger problems. The performance of the robust model is a function of the parameter η. It was shown that $\eta = \eta_c$ is the optimal choice for η. Lastly, the robust model, although tends to give conservative results, comes with a guarantee of being physically realizable and lower computational overhead compared to the two-stage linear.

Future work will consider additional optimization methods and applications and the impact of i) the grid conditions and ii) a heterogeneous fleet BESS units to understand the effect of optimization methods on the aggregate response in the context of separate batteries charging and discharging simultaneously.

REFERENCES

[1] M. R. Almassalkhi and I. A. Hiskens, "Model-Predictive Cascade Mitigation in Electric Power Systems With Storage and Renewables—Part I: Theory and Implementation," *IEEE Transactions on Power Systems*, vol. 30, pp. 67–77, Jan. 2015.

[2] K. Garifi, K. Baker, D. Christensen, and B. Touri, "Convex Relaxation of Grid-Connected Energy Storage System Models With Complementarity Constraints in DC OPF," *IEEE Transactions on Smart Grid*, vol. 11, pp. 4070–4079, Sept. 2020.

[3] J. M. Arroyo, L. Baringo, A. Baringo, R. Bolaños, N. Alguacil, and N. G. Cobos, "On the Use of a Convex Model for Bulk Storage in MIP-Based Power System Operation and Planning," *IEEE Transactions on Power Systems*, vol. 35, pp. 4964–4967, Nov. 2020.

[4] D. Pozo, "Linear Battery Models for Power Systems Analysis," Apr. 2022.

[5] M. H. Rostamiyan, M. H. Abardeh, A. A. Azarfar, M. S. Moghaddam, and N. Salehi, "A MIQP Approach Based on Demand Response in Distribution Networks to Improve the Multi-Objective Function in the Presence of Renewable Energy Resources and Batteries to the Subway Systems," *IEEE Access*, vol. 11, pp. 17603–17612, 2023.

[6] N. Nazir and M. Almassalkhi, "Guaranteeing a physically realizable battery dispatch without charge-discharge complementarity constraints," *IEEE Transactions on Smart Grid*, pp. 1–1, 2021.

[7] Z. Li, Q. Guo, H. Sun, and J. Wang, "Sufficient Conditions for Exact Relaxation of Complementarity Constraints for Storage-Concerned Economic Dispatch," *IEEE Transactions on Power Systems*, vol. 31, pp. 1653–1654, Mar. 2016.

[8] N. Nazir, P. Racherla, and M. Almassalkhi, "Optimal Multi-Period Dispatch of Distributed Energy Resources in Unbalanced Distribution Feeders," *IEEE Transactions on Power Systems*, vol. 35, pp. 2683–2692, July 2020.

[9] F. Sossan, E. Namor, R. Cherkaoui, and M. Paolone, "Achieving the Dispatchability of Distribution Feeders Through Prosumers Data Driven Forecasting and Model Predictive Control of Electrochemical Storage," *IEEE Transactions on Sustainable Energy*, vol. 7, pp. 1762–1777, Oct. 2016.

[10] E. Namor, F. Sossan, R. Cherkaoui, and M. Paolone, "Control of Battery Storage Systems for the Simultaneous Provision of Multiple Services," Oct. 2018.

[11] M. Kazemi, H. Zareipour, N. Amjady, W. D. Rosehart, and M. Ehsan, "Operation Scheduling of Battery Storage Systems in Joint Energy and Ancillary Services Markets," *IEEE Transactions on Sustainable Energy*, vol. 8, pp. 1726–1735, Oct. 2017.

[12] R. Kini, D. Raker, T. Stuart, R. Ellingson, M. Heben, and R. Khanna, "Mitigation of PV Variability Using Adaptive Moving Average Control," *IEEE Transactions on Sustainable Energy*, vol. 11, pp. 2252–2262, Oct. 2020.

[13] M. A. Syed and M. Khalid, "Moving Regression Filtering With Battery State of Charge Feedback Control for Solar PV Firming and Ramp Rate Curtailment," *IEEE Access*, vol. 9, pp. 13198–13211, 2021.

[14] T. Wang, H. Kamath, and S. Willard, "Control and Optimization of Grid-Tied Photovoltaic Storage Systems Using Model Predictive Control," *IEEE Transactions on Smart Grid*, vol. 5, pp. 1010–1017, Mar. 2014.

[15] Q. Yan, B. Zhang, and M. Kezunovic, "Optimized Operational Cost Reduction for an EV Charging Station Integrated With Battery Energy Storage and PV Generation," *IEEE Transactions on Smart Grid*, vol. 10, pp. 2096–2106, Mar. 2019.

[16] K. Divya and J. Østergaard, "Battery energy storage technology for power systems—an overview," *Electric Power Systems Research*, vol. 79, no. 4, pp. 511–520, 2009.

[17] PJM, "Ancillary services - pjm." Available at https://www.pjm.com/markets-and-operations/ancillary-services.aspx.

[18] S. Anywhere, "Solar anywhere data." Available at https://www.solaranywhere.com/products/solaranywhere-data/.

[19] J. Johnson, A. Ellis, A. Denda, K. Morino, T. Shinji, and T. Ogata, "PV Output Smoothing using a Battery and Natural Gas Engine-Generator," Tech. Rep. SAND2013-1603, Sandia National Lab, Feb. 2013.

[20] ISO-NE, "Real-time hourly lmps." Available at https://www.iso-ne.com/isoexpress/web/reports/pricing/-/tree/lmps-rt-hourly-final.

[21] T. Inc., "Tesla powerwall." Available at https://www.tesla.com/powerwall (2019/06/11).